# Effect of preferential transport and coherent denitrification on leaching of nitrate to drainage.

David Nagy[1], Annette E. Rosenbom[2], Bo V. Iversen[1], and Finn Plauborg[1]

[1]Department of Agroecology, Aarhus University, Blichers Alle 20, Tjele, 8830, Denmark. Tel.: +4552798854
[2]Department of Geochemistry, Geological Survey of Denmark and Greenland, Oester Voldgade 10, Copenhagen K, 1350, Denmark

**Correspondence:** David Nagy (davidnagy@agro.au.dk)

**Abstract.** To protect the quality of the aquatic environment, it is imperative to be able to assess the leaching of nitrate through various hydrogeological settings. Numerical model concepts have been developed in order to describe this leaching and possible routes of nitrogen at field scale, often without being evaluated in regard to their ability to account for dominant preferential transport and coherent denitrification, which is the rule rather than the exception in soils. This study evaluates whether it is

5  possible to describe 10-years of nitrate concentrations, measured in drainage from a tile-drained agricultural clay till field in Denmark, by applying the soil-plant-atmosphere model DAISY, capable of accounting for preferential transport and denitrification. A DAISY model concept, including macropores capable of capturing the water and bromide balance of the field within this specific timeframe, was able to predict the water transport to drainage, dry matter and N-yield of the harvested crops, while it was unable, with the standard default denitrification model, to predict dynamics and quantity of N-loss to drainage. This was

10  caused by a fast saturation of the plow layer, where nitrate seemed to be denitrified almost instantly, and no surplus nitrate remained to be transported to the drainage. To circumvent this and describe the measured N-loss, modification to the water reduction function affecting denitrification was conducted. The denitrification had to be reduced by approximately 50% from a seasonal average of $75 \, \mathrm{kg \, N \, ha^{-1}}$ to $35 \, \mathrm{kg \, N \, ha^{-1}}$ while 48% to 80% of the total N-loss to drainage had to be preferentially transported from the plow layer. This study therefore reveals that, by not accounting for preferential transport and coherent

15  denitrification, there is a high risk of underestimating leaching of nitrate to the aquatic environment.

**Keywords.** Preferential transport, Denitrification, Modelling, N-leaching, Drainage

## 1 Introduction

Nitrogen is an essential element of crop growth and development. The input of agricultural nitrogen fertilisers, however, is one of the most substantial causes of non-point source nitrogen pollution of surface water (including drainage) and groundwater,

20  despite the Nitrate Directive (EEC, 1991). One of the most widespread impacts on inland surface water and coastal seawater is eutrophication, which is induced by unnatural enrichment of nitrogen and phosphorus. In order to increase agricultural production from the arable land, artificial subsurface tile drains are widely deployed around Denmark to remove excess water from fields with poor natural drainage. Nevertheless, this agricultural water management measure puts the aquatic environment at

risk since it facilitates rapid nitrogen transport pathways to the aquatic environment, with limited possibilities for the reduction
25  of nitrate (Ernstsen et al., 2015) followed by eutrophication (Blann et al., 2009). Bergstrom (1995) argued that nitrate would be
transported evenly through the matrix media and probably not via preferential flow pathways. In contrast, Larsson and Jarvis
(1999) showed the importance of macropore flow in regard to nitrate transport in structured soils. Mohanty et al. (1998) found
water flow better described by using bimodal unsaturated hydraulic functions accounting for preferential flow of water, rather
than with the commonly used unimodal hydraulic functions. Recently, Cheng et al. (2014) have shown that the leaching of
30  nitrate from an undisturbed soil column of loam was, on average, 2.31 times faster than from a packed soil column. Besides
the contamination threat to the aquatic environment, agricultural fertilisation practices pose a risk as one of the accelerators
of global warming, since they are a source of nitrous oxide ($N_2O$) emission. Hofstra and Bouwman (2005) concluded, by
statistical modelling including studies with 336 denitrification measurements in contrasting crop management systems and
landscapes, that the possible magnitude of gaseous N loss was around $10\,\mathrm{kg\,N\,ha^{-1}\,yr^{-1}}$ from a well-drained field with an
35  uncertainty of 2-46 $\mathrm{kg\,N\,ha^{-1}\,yr^{-1}}$. The authors classified the results based on drainage conditions, such as well-drained and
poorly drained, with a contribution of 13 and 22 $\mathrm{kg\,N\,ha^{-1}}$, respectively. According to Knudsen et al. (2000), in Denmark, the
general "rule of thumb" for sandy clay loam and clay loam is a loss of 20-40 $\mathrm{kg\,N\,ha^{-1}\,yr^{-1}}$ due to denitrification. Besides
nitrogen being a pollution factor, nitrogen is one of the most limiting nutrients for vegetation, which regulates crop productivity
in the agricultural ecosystem. The proportion of various nitrogen compounds in the system depends both on the form and the
40  amount of the input of nitrogen (organic or inorganic), but also on transformations in the soil. Although inorganic nitrogen
is responsible for both plant production and facilitation of eutrophication, the labile N compounds account for less than 5%
of the total nitrogen in soil (Brady et al., 2008; Jarvis et al., 1996). Nitrogen is present in organic form as plant residues, but
since it is not soluble in water, plants have limited access to this storage. Microorganisms (bacteria and fungi) convert the
organic nitrogen into ammonium and nitrate (mineralisation), and this inorganic nitrogen can be mobilised by the root system
45  of plants. The excess available inorganic nitrogen is either transported to surface waters by subsurface tile drain systems or the
groundwater, if it is not immobilised or denitrified (Reddy and Ronald, 2008). Today, models applied to assess the water and
solute transport include discrete representation of soil layers which, with their hydraulic, chemical and biological properties,
drive the organic and inorganic compounds through the simulated soil profile (Manzoni and Porporato, 2009). Such models
are often one-dimensional and apply Richard's equation (Richards, 1931) paired with the advection-dispersion equation, and
50  depict the subsurface drain transport with the widely used Hooghoudt equation (Hooghoudt, 1940). Besides the equilibrium
water and solute transport, several of these models have included preferential pathways in order to simulate the rapid transport
throughout the soil media (Simunek et al., 2003). The ability of these models to describe preferential transport and coherent
denitrification in relation to leaching of nitrate has however seldom been evaluated in detail, which is imperative in order to
protect the aquatic environment against nitrate pollution. The objective of this study was to evaluate, by using one-dimensional
55  physically-based root zone model DAISY (Hansen, 2002), the effect of preferential transport and denitrification on leaching
of nitrate to drainage during a 10-years period as measured for an agricultural clay till field included in the Danish Pesticide
Leaching Assessment Programme (PLAP; Lindhardt et al. (2001); web address: http://pesticidvarsling.dk). This was conducted
by (a) testing the performance of the preferential flow and transport model concept developed by Nagy et al. (2019) for this

specific field, in describing the measured loss of nitrate to drainage, and (b) improving this model performance by optimising
60  the concept regarding sensitive, hydraulic, crop nitrification and denitrification parameters (Hansen et al., 2012a).

## 2 Material and Methods

### 2.1 Long-term field experiment

The experimental field (1.69 ha) has been included in PLAP and is located in Silstrup (56 °55'56 "N 8 °38'44"E) in the North
West of Denmark (Lindhardt et al., 2001) (Fig. 1). The field was set up in 1999, with the knowledge that since 1942 the field
65  had been used for agricultural purposes and was artificially drained in 1966 with a systematic and uniform layout of the drain
pipe system. The field was farmed from 1983 without the use of plot experiments and, since the monitoring started in 1999,
the field has been cultivated with crops in a rotation following Danish standard agronomic procedures concerning soil tillage,
fertilisation and spraying with pesticides. The field and the surrounding area are dominated by Weichselian glacial clay till
deposits in mixture with thin meltwater sand lenses. The field is heavily fractured and contains a high density of macropores.
70  In the top 1 m, traces of agricultural processes are highly visible, dominated by bioturbation and desiccation cracks, and
the macropore density was approximated to 400 pores $m^{-2}$ (Lindhardt et al., 2001) with diameters of 2-5 mm, utilising the
methodology from Klint and Gravesen (1999). The most common horizon subdivision is between the topsoil, or plow layer
($A_p$ horizon), and subsoil (B horizon) with average depths of 31 cm and 140 cm, respectively. The textural evaluation showed
a plow layer with 18-25% clay and an even more varying clay content within the underlying soil of up to 43%. The loss of
75  pesticides has from the start of the monitoring program been followed by flow proportional sampling of water from the drainage
system and grab samples of water from deep groundwater wells, installed at the border of the field. In addition to pesticide
leaching assessed from the water samples, nitrate concentration in the same water samples have also been measured. Further
details on the monitoring program are given by Lindhardt et al. (2001). In the present study, Silstrup data is included from the
period 2000-2010. Silstrup has an average yearly precipitation of 838 mm. The groundwater table is located relatively deep for
80  the duration of the dry seasons with a depth of 2-4 m, whereas during the wet season it varies between $0.5 - 1.5$ m. On average,
the drainage was occurring 168 days per year with a mean magnitude of $0.5$ $mm\,d^{-1}$ corresponding to 8.45 $m^3\,d^{-1}$ from
the whole field. Most of the drainage occurred during the wet season (late autumn and winter), although occasional sudden
preferentially induced flow was observed during the spring and summer period. Further hydrological details can be found in
Nagy et al. (2019) and Lindhardt et al. (2001).

85  [Figure 1 is about here]

Management and measurements: From 2000 through 2010, crops of spring barley (SB) and winter wheat (WW) were grown in
rotation with winter rape (WR), fodder beets (FB), pea (P), and maize (M) (Fig. 2). No catch crop has been cultivated. Every
single year, the total amount of N fertilisers applied was adjusted to accommodate the selected crop, considering the nutritional
effects of the previous crops in rotation. On average for 2000–2010, the annual N-application was 197 $kg\,N\,ha^{-1}\,yr^{-1}$. The
90  climate data was recorded from 29 April 2000 until 31 December 2010 on an hourly basis. The data include wind speed [$ms^{-1}$],

global radiation [$\mathrm{W\,m^{-2}}$], air temperature [$^\circ$C] and vapour pressure [Pa] to be able to determine the evaporative demand utilising the Penman-Monteith Reference Evaporation equation (Allen et al., 1998). The wind speed measurements at 10 meters height were scaled to 2 meters, assuming a logarithmic wind profile and neutral atmosphere (Allen et al., 1998). Hourly precipitation [mm] was sampled with a tipping bucket gauge (Lambrecht meteo GmbH) at the upper North East end of the field

95 (Lindhardt et al., 2001; Nagy et al., 2019). At the tile drain outlet, hourly drainage discharge was measured using the Thompson weir method (Lindhardt et al., 2001). ISCO samplers (Teledyne ISCO, Lincoln, NE, USA) had been utilised to get samples of drainage water. Drainage water was sampled time proportionally (hourly) until 2004 and thereafter sampled proportional with sub-samples collected for every 3000 L of drainage flow during the winter months (September–May) and 1500 L during the summer season (June–August). Each week, all the collected sub-samples were pooled, and a sample was analyzed for nitrate,

100 in the laboratory (Ernstsen et al., 2015). The soil water was sampled with PRENART SUPER QUARTZ suction cups (Prenart, DK)) consisting of porous Polytetrafluoroethylene (PTFE) mixed with quartz. Four suction cups were installed at a depth of 1 m and four at a depths of 2 m at the edge of the field (Lindhardt et al., 2001). The sampling bottles are 1- or 2-liter glass bottles, and samples were taken every 7 days. N-concentration and transport: In the period 2000–2010, the nitrate-N concentrations in drainage at Silstrup varied between 0.5–34 $\mathrm{mg\,N\,L^{-1}}$ and, for 20 percent of the time, exceeded the European limit for drinking

105 water (Fig. 2). Slightly elevated nitrate-N concentrations were measured during M2002 (15.47 $\mathrm{mg\,N\,L^{-1}}$), P2003 (13.96 $\mathrm{mg\,N\,L^{-1}}$), WW2006/2007 (12.68 $\mathrm{mg\,N\,L^{-1}}$) and in extreme WW2004/2005 (22.10 $\mathrm{mg\,N\,L^{-1}}$), FB2008 (34.29 $\mathrm{mg\,N\,L^{-1}}$) was two and three times more than the allowed EU limit for drinking water supply (11.3 $\mathrm{mg\,N\,L^{-1}}$). Most of the N leaching occurred throughout the fall- and wintertime, and generally, the daily fluxes were below 1 $\mathrm{kg\,N\,ha^{-1}\,d^{-1}}$. For a short period of time, the concentration hit the range of 1–2 $\mathrm{kg\,N\,ha^{-1}\,d^{-1}}$ and has hardly ever been above 2 $\mathrm{kg\,N\,ha^{-1}\,d^{-1}}$ (Fig. 2). The

110 yearly drainage transport of nitrate-N coming from the field was between 3– 23 $\mathrm{kg\,N\,ha^{-1}\,yr^{-1}}$, corresponding to 1–16% of the annually applied N fertilisers (Fig. 2). Even though N was applied every year at nearly the same plant development stages, no immediate effects on nitrate-N concentrations in the drainage were observed. This applied to both mineral and organic N fertilisers (Ernstsen et al., 2015). Figure 2 presents the water and $NO_3$-N leaching accumulated seasonally. One season ran from April 1st of the given year until March 31st of the next year to represent the significant crop growing and N fertilisation season.

115 This seasonal approach is an alteration from the standard use of the hydrological year, as United States Geological Survey (USGS) defines it, the period between October 1st of one year and September 30th of the following year (U.S.G.S, 2016).

[Figure 2 is about here]

## 2.2 The DAISY-model

DAISY is a one dimensional physically-based root zone model, being able to model water balance, carbon and nitrogen

120 turnover, solute balance, heat balance and crop production based on input of climate data, soil texture, and various management strategies (Hansen, 2002). The water balance includes surface and subsurface matrix and preferential flow processes, as well as plant uptake and flow to tile drains. It puts great emphases on nitrogen balance and modelling of processes in the nitrogen

cycle, mineralisation-immobilisation, nitrification, and denitrification. Further, it simulates uptake and leaching of ammonium
and nitrate to drains and groundwater (Hansen et al., 2012a).

125    *Soil hydraulics:* DAISY uses the Richards equation to solve the one-dimensional water transport in the matrix.

$$\frac{\delta\theta}{\delta t} = \frac{\delta}{\delta z}\left[K\frac{\delta\psi}{\delta z}\right] + \frac{\delta K}{\delta z} - S \tag{1}$$

,where $\theta$ [VV$^{-1}$] is the volumetric water content in the soil, $\psi$ [L] is the soil water pressure potential, $K$ [LT$^{-1}$] is the hydraulic
conductivity of the soil and S is a sink term, which represents the loss to the drain, macropore or plant water uptake. In order
to solve the Richards equation, in this study, the van Genuchten (vG) soil water retention model was used (Van Genuchten,
130    1980).

$$\theta = \begin{cases} \theta_r + \frac{\theta_s - \theta_s}{[1+|\alpha\psi|^n]^m} & ; h < 0 \\ \\ \theta_s & ; h > 0 \end{cases} \tag{2}$$

, where $\alpha$, $n$ and $m$ are empirical shape parameters, and $\theta_s$ and $\theta_r$ are the saturated and the residual water content respectively
of the given soil. In this study, the van Genuchten model is coupled with the Mualem hydraulic conductivity theory (Mualem,
1976) (vGM), where $m$ is achieved as $m = 1 - n^{-1}$. The Mualem hydraulic conductivity is expressed as

135    $$K = K_{sat}S_e^l\left[1 - (1 - S_e^{m^{-1}})^m\right]^2 \tag{3}$$

, where $K_{sat}$ is the hydraulic conductivity at saturation , $S_e$ is the effective saturation, which is calculated as, $S_e = \frac{\theta - \theta_r}{\theta_s - \theta_r}$ and
$l$ is the shape form, which represents the pore connectivity.

The fast flow domain in DAISY is described by a macropore module designed by Mollerup (2010) and tested in technical
reports, prepared for and published by the Danish Environmental Protection Agency (Hansen et al., 2010a, b, 2012b). The
140    macropore is a vertically oriented feature in the DAISY model, characterised by physical properties such as length, diameter
($d$) and density ($\rho$). The macropore flow is initiated when the matrix pressure exceeds a specific pressure potential called $\psi_{init}$.
If this pressure potential is exceeded, the macropore domain activates and water starts to fill up the macropore. When the
pressure potential drops below a level called $\psi_{term}$, the macropore flow is terminated. In a specific case, when a macropore
is filled with water, it can be transferred back to the soil matrix at a certain point. It is initiated when the pressure difference
145    between the macropore and the matrix exceeds a minimum pressure barrier $\psi_{barrier}$. All pressure parameters are common for
all macropore classes. Macropores can be drain ended and matrix ended macropore, where the drain ended macropore has no
water build up, because when the water enters into the macropore, it is instantaneously transported to the drain. In contrast,
in the matrix macropores, the water has the availability to build up and be transported back to the matrix later, as discussed
above. More details of the mathematical and physical description of the macropore domain can be found in Mollerup (2010).
150    *Soil N pools:* Nitrogen (N) is present in two different fractions in the soil as organic or inorganic forms. These two fractions are
in a constant exchange with each other, through mineralisation and immobilisation. According to Jarvis et al. (1996), inorganic
N represents approximately 5% of the total soil N, although it may change after fertilisation for a short period. Hence, organic

N, which occurs in many forms, including proteins, urea, amino and nucleic acids and nucleotides is by far the largest N
fraction of the soil.

155                                        [Figure 3 is about here]

Although the microbial state of N may cover only 3-5%, most of the transformation processes (mineralisation, immobilisation,
and denitrification) are mediated by the microbial community. In DAISY, soil N is divided into six different pools (Fig. 3), and
some N is in an inert pool (not shown in Fig. 3). The pools are separated into two distinct groups, pools with slow turnover
rate (denoted 1), and pools with higher turnover rate (denoted 2). Thereby the soil organic matter pool 1 (SOM1) mainly

160    contains chemically stabilised compounds which are relatively resistant to biological degradation. The other organic matter
pool (SOM2) is physically stabilised and more labile, although temporarily resistant to biodegradation due to sorption to soil
colloids. Added organic matter refers to manure, crop residue or green manure and is typically divided into AOM1 – cell wall
material and AOM2 cell extractable substances. The main driver of the C/N turnover is the soil microbial biomass (SMB),
which controls the turnover processes of the dissolved organic matter, even though it only represents a small quantity of the

165    total organic matter (Hansen, 2002). _Mineralisation-immobilisation turnover:_ Net N mineralisation or net N immobilisation is
determined by the microbial activity and the overall N balance. If the content of N in the assimilated organic substance is higher
than that required by the biomass for growth, ammonium is excreted to the soil solution. On the other hand, if the content of N
in the assimilated organic substance is lower than that required by the biomass for growth, ammonium or nitrate is assimilated
from the soil solution and transformed into nitrogenous organic compounds (Hansen, 2002). The measure used in DAISY for

170    the available organic substrate is the content of carbon in the organic matter. Hence, the simulation of net mineralisation of
N is based on the simulation of the turnover rate of soil organic carbon. The potential decomposition rate of organic carbon
in various pools in the soil is described by first-order kinetics, but is affected by the abiotic factors (soil water content, soil
temperature, pH (5 to 8), oxygen pressure) and availability of inorganic N. The potential N mineralisation rate is strongly
related to the carbon turnover, as every sub-pool has a C:N ratio and the decomposition of carbon leads to mineralisation of

175    N carbon according to this ratio. Hence, the potential background N mineralisation from dead native organic matter in the
soil is highly dependent on the distribution of the dead native soil organic matter between SOM1 and SOM2, which in turn is
strongly related. By default, the C:N ratio for SMB1 and SMB2 is assumed to be 6 and 10, respectively, however, it can be
specified differently if required. _Denitrification:_ In the present model, denitrification is simulated using a rather simple index
type model considering the decomposition of organic matter, volume of anaerobic microsites expressed simply in terms of soil

180    water content, soil temperature, and the concentration of nitrate in soil solution. This is a typical way of using a simplified
model for denitrification (Eq. 4), according to Heinen (2006):

$$D_a = \alpha_d f_N f_S f_T f_{pH} \tag{4}$$

,where $D_a$ is the actual denitrification rate, $\alpha_d$ represents the potential but may in different models have different formulation,
$f_N$ is a dimensionless reduction function for nitrate content in soil or represents the nitrate content in the soil (depending

185    on the exact formulation determined by $\alpha_d$), $f_S$ is a dimensionless reduction function for water content in the soil, $f_T$ is a

dimensionless reduction function for temperature in the soil, and $f_{pH}$ is a dimensionless reduction function for soil pH. The $\alpha_d$ parameter can be considered in two ways, depending on the model concept; either $\alpha_d$ represents the potential denitrification rate $D_p$ (same units as $D_a$) or it represents a first-order denitrification coefficient (constant) $k_d$. In both cases, $\alpha$ can be a constant parameter or can be related to carbon dynamics. In the DAISY model, the potential denitrification rate (in case of
190 anoxic conditions and sufficient nitrate concentration in the soil solution) is expressed as a linear function of the $CO_2$ evolution rate:

$$\xi_d^* = \alpha_d^* \xi_{CO_2} \tag{5}$$

,where $xi_d^*$ is the potential denitrification rate of the soil, $xi_{CO_2}$ is the $CO_2$ evolution rate simulated by the mineralisation - immobilisation - turnover model (MIT-model), and $\alpha_d^*$ is an empirical constant, which was taken from Lind (1980), who
195 measured the relationship between easily decomposable organic matter and denitrification capacity. The actual denitrification rate is determined either by the actual microbial activity at the anaerobic microsites, or the transport of nitrate to the anaerobic microsites represented by the left and right solution, respectively, in Eq. (6). In the case of ample supply of nitrate, the actual denitrification rate is determined by multiplying the potential denitrification rate by a modifier function. Hence, the actual denitrification can be simulated as:

200 $$\xi_d = min\{f_T f_S \xi_d^*; K_d N_{ni}\} \tag{6}$$

,where $xi_d$ is the actual denitrification, $K_d$ is an empirical proportionality factor when denitrification is governed by the microbial activity at the anaerobic microsites and $N_ni$ the nitrate concentration in the soil. The maximum transport of nitrate to microsites can be assumed to be relative to the nitrate concentration in the soil ($N_{ni} = \theta C_{ni}$, where $C_{ni}$ is the concentration in the soil solution, and $\theta$ is the soil water content). In Eq. (6), the modifier function $f_S$ is assumed to be a function of the soil
205 water content. Many models use a power reduction function of the form (Grundmann and Rolston, 1987):

$$\begin{cases} 0 & ; S < S_t \\ \left(\frac{S - S_t}{S_m - S_t}\right)^w & ; S_t \le S \le S_m \\ 1 & ; S_m < S \end{cases} \tag{7}$$

,where $f_S$ is the dimensionless power water reduction function in the range [0, 1], $S$ is the dimensionless degree of water saturation or water-filled pore space; $S$ is always in the range [0, 1], $S_m$ is close to full water saturation above which $f_S$=1, $S_t$ is a threshold value for S below which $f_S$=0, $w$ is a curve shape parameter determining the steepness of the curve (Heinen,
210 2006). The temperature modifier function $f_T$ is an Arrhenius like function (Rodrigo et al., 1997) by correlating the exponential rate of biological processes to the increasing temperature. According to Heinen (2006), based on a sensitivity test on Eq.(4), $f_S$ is the most sensitive within all modifiers. Therefore, this study is only focusing on the water saturation effect on denitrification in the aspect of calibration Eq.(4).

## 2.3 Initial model concept

215 Nagy et al. (2019) conceptualised the water and solute transport for the clay till field Silstrup with three different macropore settings and three different horizons (A, B and C). The macropore settings included vertical macropore transport supplying water directly to 1) the drainage pipes, 2) to drainage pipes and the matrix 3) to drainage pipes and the matrix added with fractures, supplying water to the matrix in the saturated zone. The best-calibrated concept with drainage ending macropores (DM1, DM2) and matrix (MM1, MM2, MM3) ended macropores (Fig 4a), yielded indices for the evaluation of measured and

220 simulated drainage, 0.12/0.48 nMAE (normalized Mean Absolute Error) and 0.87/0.82 KGE (Kling –Gupta Efficiency) and for the bromide drainage transport 0.14/0.85 nMAE with 0.85/0.52 KGE. Further details in Nagy et al. (2019) (Fig. 4b, 4c).

[Figure 4 is about here]

## 2.4 Objectives included in the automated calibration procedure

The soil and hydrological parameters are adjusted in order to improve the bromide ($Br^-$) transport as in the hydrological model

225 by Nagy et al. (2019), which was not calibrated on $Br^-$ transport. A better performance of the model could particularly be expected just after the application of $30\,\mathrm{kg\,KBr\,ha^{-1}}$, corresponding to $20.14\,\mathrm{kg\,Br\,ha^{-1}}$ (cf. Fig. 9 in Nagy et al. (2019)). Therefore new objectives have been included in the calibration procedure, such as the harvested dry matter yield - *DM yield*, harvested N yield - *N yield*, N drainage flux dynamics - *ND* $[\mathrm{kg\,N\,ha^{-1}\,h^{-1}}]$ and cumulative N transport - *NC* $[\mathrm{kg\,N\,ha^{-1}\,h^{-1}}]$, $Br^-$ transport dynamics – *BRD1* $[\mathrm{kg\,Br\,ha^{-1}\,h^{-1}}]$ and cumulative transport – *BRC1* for the whole tracer experiment period

230 $[\mathrm{kg\,Br\,ha^{-1}\,h^{-1}}]$, $Br^-$ transport dynamics – *BRD2* $\mathrm{kg\,Br\,ha^{-1}\,h^{-1}}]$ and cumulative transport – *BRC2* $[\mathrm{kg\,Br\,ha^{-1}\,h^{-1}}]$ for the period of initial $Br^-$ breakthrough (1 April 2000 - 1 June 2000) and to not compromise the earlier findings from Nagy et al. (2019), the drainage dynamics - *DD* $[\mathrm{mmh^{-1}}]$ and cumulative transport – *DC* $[\mathrm{mm}]$ including soil water content measurement $[\mathrm{cm^3\,cm^{-3}}]$ at depth 25cm - *S25* and 60cm - *S60* were included. According to Muleta (2011) and Nagy et al. (2019), the mean absolute error was used for calibration. Since the model was constrained to different objectives with different units, the

235 objectives in Eq.(8) were normalized by means of the corresponding observations in order to aggregate them into one objective function, which is eligible for automated calibration (Criss and Winston, 2008; Nagy et al., 2019).

$$nMAE_{season}^{obj} = \frac{\frac{1}{N}\sum_{i=1}^{N}\left|sim_{season,i}^{obj} - obs_{season,i}^{obj}\right|}{\overline{obs_{season}^{obj}}}; obj = \{ND, NC, DD, DC, S25, S60\} \tag{8}$$

,where N is the number of observations of a given objective within a year and

$$\overline{obs_{season}^{obj}} = \frac{1}{N}\sum_{i=1}^{N}obs_{season,i}^{obj} \tag{9}$$

240

$$\overline{nMAE^{obj}} = \frac{1}{K}\sum_{k=1}^{K}nMAE_{season,i}^{obj} \tag{10}$$

,where k is the number of calibration years. Due to *DM yield* and *N yield* having only one value per season, a seasonal aggregation is not possible. Thus, nMAE was calculated for all seasons and normalized by means of the observations. The same applied to the Br⁻ (*BRD1*, *BRC1*, *BRD2*, *BRC2*) objectives due to the tracer experiment being held for one season in

245  2000-2001. The multi-objective function calculated for the automated calibration is expressed as:

$$nMAE^{final} = \sum \overline{nMAE^{obj}}; \qquad obj = \left\{ \begin{array}{c} N\,yield, DM\,yield, ND, NC, \\ BRD1, BRC1, BRD2, BRC2, \\ DD, DC, S25, S60 \end{array} \right\} \qquad (11)$$

For further evaluation purposes nRMSE[%] (normalized Root Mean Squared Error), normalized on the difference on the minimum-maximum deviation of the observation and KGE (Kling-Gupta efficiency measure were calculated. KGE is presented by Gupta et al. (2009)). Singh et al. (2005) and Hansson and Hokfelt (1975) suggested that if MAE or RMSE of the model is

250  lower than half of the standard deviation (SD) of the measured data, the model may be considered as an adequate representation of the measured data. On the other hand, KGE with a range of $-\infty$ to 1, if KGE is above 0.5, the model can be considered as satisfactory.

## 2.5  Parameters

The hydrological parameters were taken from Nagy et al. (2019) as it is considered to be a reasonable baseline for the calibration

255  (Table 1 and 2). All initial hydraulic parameters represented presented in Table 1, and 2 were given a ±5 % uncertainty boundary range in order to see which parameter would be influential on the "new" objectives.

[Table 1 is about here]

For the fast flow domain, the macropore model of DAISY using the conceptualisation of Nagy et al. (2019) was applied (Table 2).

260  [Table 2 is about here]

To be able to evaluate the model behaviour considering the "new" objectives conditions, one has to determine essential input parameters important for calibrating N loss by crop harvest, nitrate leaching and gaseous $N_2$ loss due to denitrification (Table 3). Only crop parameters influencing dry matter formation were selected, as the data available did not allow a calibration of the N uptake parameters.

265  [Table 3 is about here]

The simple photosynthesis description in DAISY requires a value for maximum assimilation rate ($F_m$) [$g\,CO_2\,m^{-2}\,h^{-1}$], quantum efficiency($Q_{eff}$) [$(g\,CO_2\,m^{-2}\,h^{-1})(W\,m^{-2})^{-1}$] at low light, and a temperature factor for assimilating production, referred to as a piece-wise linear function (PLF) (Hansen et al., 2012a; Vries, 1989). Also, to get more control over the crop production the conversion efficiency (growth respiration) ($E$) [$(g\,CH_2O)(g\,DM)^{-1}$] (Manevski et al., 2016; Vries, 1989) was

270  taken into the calibration besides the Photosynthetic Active Radiation extinction coefficient ($Par_{ext}$) and the temperature

sum at emergence ($T_{sum}$, Table 3). Additionally, the crop uptake reflection factor of Br⁻ ($CURF_{BR}$, (Hansen, 2002)), the SOM fraction ratio of the plow layer ($SOM_{ratio}$) which describes the ratio SOM1:SOM2 has been added as a parameter, as well as parameters from the denitrification module for both fast and slow pools: the anaerobic denitrification constant ($\alpha_d^*$) [$(\mathrm{g\,NO_3 - N\,h^{-1}})(\mathrm{g\,CO_2 - C\,h^{-1}})^{-1}$] and the empirical proportionality factor ($K_d$) from Eq.(5) and Eq.(6), respectively, and

275    $S_t$ and $w$ from Eq.(7) (Table 4).

[Table 4 is about here]

The initial values of the selected crop and denitrification parameters were based partly on the values recommended for DAISY in the model library (https://DAISY.ku.dk/, Hansen et al. (2012a)) and on literature screening. Due to the lack of data on the crop growth, N uptake, and partitioning during the growth season, no extensive calibration of the crop models was possible.

280    **2.6    Sensitivity analysis**

The range of crop parameter values is biologically constrained by the diversity of crops and their cultivars. Given the lack of knowledge associated with the range of the variability that is genetic for most of the crop model parameters, uniform distribution for each parameter was assumed with ±20% uncertainty bound except $Par_{ext}$ where the bounds were set ±50%. All denitrification related parameters were given ±10% uncertainty bounds except for the water reduction function, the ranges

285    for which were taken from Heinen (2006). The SOM fraction ratio varied within from 0.43 to 2.33, which indicate fractions of SOM1:SOM2 as 0.3:0.7 to 0.7:0.3 and $CURF_{BR}$ could vary from 0 to 1, where 1 means no crop uptake. Key parameters directly related to crop development, leaf photosynthesis, and net mineralisation of plow layer as one of the input source of denitrification, were tested for sensitivity by the Morris sensitivity screening (Campolongo et al., 2007; Morris, 1991; Nagy et al., 2019) in order to help in finding sensitive parameters that have the most influence on objectives presented in section

290    2.4. The results of the sensitivity screening were turned into the Morris distance($\epsilon$) (Ciric et al., 2012; Jabloun, 2015), which represents the Euclidean distance of the parameter from (0,0) on the $\mu^*$-$\sigma$ coordinate system (Campolongo et al., 2007). The decision on sensitivity threshold was made by K-Means Clustering (Jain and Dubes, 1988). For each objective, the parameters were clustered into 3 groups (Low, Medium, High) by its $\epsilon$.

**2.7    Calibration methodology**

295    The overall objective function was based similar to the mathematical formulation, which was used in Nagy et al. (2019), by calculating the normalized Mean Absolute Error of each objective described in section 2.6 annually for the period of 2000-2007. In order to stabilise the N dynamics, 4 years were run prior to 2000 as a warm-up period. The calibration of the model was done by differential evolution (DEoptim, Ardia D. (2016)) in conjunction of RDAISY R package [under development] and RDAISY toolbox (Jabloun et al., 2014).

## 3 Results and discussion

### 3.1 Sensitivity screening results

Overall six soil matrix parameters per horizon (A, B, C), the SOM ratio for the A horizon plus two horizon depth parameters, two macropore parameters per macropore type (DM1, DM2, MM1, MM2, MM3), two soil water pressure parameters for macropores, four denitrification parameter per pool (slow/fast) and one Br⁻ parameter called soil-hydraulic parameters (SH) and eight parameters per crop as crop parameters (CP) were tested for sensitivity. All parameters were selected as a sensitive parameter, which belongs to group High, in at least one of the objectives (Fig. 5). However, to put more emphasis on the *ND* and *NC* objectives, parameters which belonged to sensitivity group Medium of *ND* and *NC* were also selected as sensitive and added to the calibration parameters (Fig. 5). All selected parameters which were involved in sensitivity analysis against 12 objective functions were listed with their associated sensitivity group (Fig. 5). Parameters with black letters are the selected sensitive parameters and with gray letters the non-sensitive. Even though a large number of parameters have been evaluated, only 16 CP and 21 SH parameters showed to be sensitive to the objective functions. All the sensitive CP parameters were, as expected, sensitive to *N yield*, since all crop parameters are related to crop growth and therefore directly affecting the crop N uptake.

[Figure 5 is about here]

SH parameters showed more diversity regarding sensitivity towards the objectives. This is in contrast to CP parameters, which mainly were sensitive towards *N yield* and *DM yield*. There was no single parameter which showed to be sensitive for all objectives. Only one SH parameter, $S_t$, affecting the denitrification reduction factor, had an effect on *DM yield* (Fig. 5). As also seen in Figure 5, no matrix and macropore SH parameter was sensitive in the objective function for *DM yield*. Therefore, it can be inferred that the crops were not affected by water stress. Furthermore, no macropore SH parameters were sensitive in the objective functions for *DM yield* and *N yield*. Even though the uncertainty bound was only ±5 % for the SH macropore parameters, the N dynamics, and quantity objectives (*ND*, *NC*) showed no sensitivity on the preferential transport. This could mean that the N transport is not affected dramatically by the preferential transport change, although earlier studies showed macropore influences on water and solute movement (Larsson and Jarvis, 1999; Nagy et al., 2019). However, the denitrification parameter, $S_t$, showed one of the highest impacts on *NC* objective, which represents the N quantity in the drainage water. This high sensitivity might be related to the fact that the denitrification is limiting the amount of NO₃-N, which would be transported by hydrological means.

### 3.2 Model calibration

Through the calibration procedure, it was found that the ND and *NC* objectives were not responsive to the initially selected crop and hydraulic parameters. Since the Br⁻ transport in the drainage simulated by the baseline model showed agreement to the accumulated measured transport, with underprediction of initial breakthrough after spraying of KBr (Fig. 4). The simulated Br⁻ uptake by FB was verified by Nagy et al. (2019); thus, the solute leaching to the groundwater seems to approximate well

to reality. If all these conditions are probable, $NO_3$-N can be only limited by gaseous loss; therefore, the denitrification model parameters had to be involved in the sensitivity and calibration process.

[Table 5 is about here]

335 As mentioned above, the sensitivity and the calibration process were done by minimising the mean nMAE performance measures. For a broader evaluation, KGE and nRMSE[%] are also presented in Table 5. The calibrated objective results show that significant improvements were achieved in all solute transport accounts (*BRD1*, *BRC1*, *BRD2*, *BRC2*, *ND*, *NC*), without compromising any of the water balance objectives (*DD*, *DC*, *S25*, *S60*). By observing the *N yield* and *NC* objectives, one can see that N transport *ND* was improved without creating nitrogen stress in the crop. Br⁻ transport improved during the tracer ex-

340 periment period, as the model was able to provide a reasonable fit for the initial breakthrough (*BRD2*, and *BRC2*, Table 5, Fig. 6). Table 6 shows the calibrated parameters and their initial value. There was no substantial change within the SH parameters. The $SOM_{ratio}$ increased, the SOM1 became 0.63, and SOM2 became 0.37 from the initial 0.5.

[Table 6 is about here]

The most significant changes appeared for parameters directly related to the denitrification reduction function ($S_{t,fast}$, $w_{fast}$,

345 $S_{t,slow}$, $w_{slow}$; Table 6), which may indicate that the default reduction function in DAISY overestimated this type of N loss.

## 3.3 Water and bromide transport

[Figure 6 is about here]

The improvement of Br⁻ transport yielded a larger initial breakthrough (Fig. 6) without compromising the water balance. The Br⁻ transport mainly responded to the change of the matrix pore distribution (van Genuchten "n") in the horizon of A and B

350 ($n_A$ and $n_B$, Fig. 5), although it could be the result of the interaction of multiple parameters.

[Figure 7 is about here]

The crop uptake reflection factor increased only slightly from 0 to 0.34 %. The FB dry matter yield decreased from 14.5 $\mathrm{Mg\,DM\,ha^{-1}}$ to 13.7 $\mathrm{Mg\,DM\,ha^{-1}}$. However, the Br⁻ uptake in fodder beet increased from 11.6 $\mathrm{kg\,Br\,ha^{-1}}$ to 12.1 $\mathrm{kg\,Br\,ha^{-1}}$, which resulted in a 2% (0.5 $\mathrm{kg\,Br\,ha^{-1}}$) higher Br⁻ uptake of the initially sprayed 20.1 $\mathrm{kg\,Br\,ha^{-1}}$. The 0.5 $\mathrm{kg\,Br\,ha^{-1}}$ pro-

355 portionately removed from all Br⁻ leaching routes and macropore leaching remained at the same magnitude. Therefore, it can be inferred that the matrix and macropore interchange did not change significantly (Fig. 7).

## 3.4 Nitrogen transport and harvest

Considering the calibrated Br⁻ transport, the overall leached quantity of Br⁻ did not change substantially. This contrasted with N transport, which responded differently to the calibration. The original model captured the N dynamics, and in one instance

360 the magnitude, of the cumulated transport during the WW2003-2004 season. The application of N fertilisers was not reflected in simultaneous or subsequent increases of N flux from the field, as well as there being no significant additive effect from crop type identified.

[Figure 8 is about here]

Figure 8 shows that the denitrification in the original model significantly outweighed the N loss by drains (measured $NO_3$-N)
with one order of magnitude with an average seasonal loss of 75 kg N ha$^{-1}$ (18 - 151 kg N ha$^{-1}$), due to denitrification from
slow and fast pools combined. Hence, it seems that denitrification limited the amount of N transported to the drainage. Nagy
et al. (2019) discovered that most of the water build up was above the plow pan in the A horizon. This could lead to this rapid
denitrification, according to Eq.(4) to Eq.(7) where one of the modifying components is the $f_S$ water factor. In DAISY, $f_S$ had
been set as default in order to increase linearly from 0 to 1 as a function of S from 0.7 to 1.0 (Hansen, 2002) (Fig. 9). This
linearity does not fit the real condition for denitrification, since the stagnation of the water above the plow pan, as it presented
in Nagy et al. (2019), should allow the N almost instantaneously to denitrify. In the calibrated model, $f_S$ dynamics based on
Eq.(7) have been changed, which resulted in a steeper reduction of the denitrification (Fig. 9). By allowing the separation of
the reduction factor for both the fast and the slow pool, the calibration of the model showed that the denitrification from the fast
pool was shrunk to the range approx. from 0.9 to 1.0 relative saturation, while the slow pool remained like the default version
of DAISY.

[Figure 9 is about here]

The modified $f_S$ showed a high impact on the N leaching, as the reduced denitrification enabled the model to depict the amount
of N transported to the drain. The main increase appeared in the directly connected macropore flow (DM1 flow, cf. Fig. 4.),
which mainly drained water from the A horizon. Since the mineralisation process is faster from the fast pool, the available
mineral N was not readily reduced to gaseous N, but instead transported through preferential pores to the drain. The average
seasonal denitrification was reduced to 34 kg N ha$^{-1}$ ($9-62$ kg N ha$^{-1}$), a reduction of more than 55% percent , which instead
was made available for crop uptake, flow to the drainage system or the groundwater. The harvested DM and N did not show
significant differences before and after calibration (Fig. 10). Some crop N and DM yield were closer to the measured values
after calibration, but although the surplus of N was increased by the lowered denitrification, this additional N was not taken
up by the crops. Overall, the objectives of *DM yield* and *N yield* were improved with the modified crop parameters (cf. Table
6 and Fig. 10). However, none of the models showed a satisfactory match for N yield. For both the original and the calibrated
model, the comparison between measured and simulated N yield showed differences of more than 10 kg N ha$^{-1}$ and even 20
kg N ha$^{-1}$ for maize in 2002 and winter wheat in 2007. As earlier stated, a calibration of the N uptake parameters in the crop
models governing the N uptake during the season was not possible, as the data available did not contain samples of biomass
and hence N uptake during the season.

[Figure 10 is about here]

### 3.5   Evaluation of the model performance related to nitrogen loss routes

The period 2007-2008 involving crop rotations of WW2006-2007 and FB2008 was selected to test the performance of the
calibrated model in simulating N transport to drains and loss to groundwater. Season 2009-2010 was excluded from the evalu-
ation since a few water balance discrepancies were discovered. Some of the precipitation input and drainage transport was not

aligned or missing , so the measured values could not be reliable. Besides data from this calibration independent evaluation period, data series of N concentration sampled with suction cups at depths of 1 m and 2 m for the period from 2000 to 2010 were used to validate the N transport to both drainage and groundwater.

### 3.6 Nitrogen transport in drainage water and deep leaching to groundwater

400 The N flux was remarkably improved according to all performance measures for the period 2007-2008 (Fig. 11). For the original modelling of the two cropping seasons, the average KGE was below zero, indicating that the observed mean N flux was better predicted than the simulated one. In contrast, the calibrated model gave satisfactory results with KGE of 0.56 and 0.5 for the objective *ND* and *NC*, respectively, which in the case of solute transport modelling is an excellent result (Hansson and Hokfelt, 1975; Singh et al., 2005). Although the comparison for the drainage season 2008-2009 was improved even after
405 calibration, less N loss to the drain system was simulated. The difference in simulated and measured N uptake in FB could not explain this difference.

[Figure 11 is about here]

The loss due to denitrification has changed similarly for the calibration period 2000-2007 from seasonal 75 to 35 $\mathrm{kg\,N\,ha^{-1}}$, which is approximately a 50 % percent reduction in total. In season 2007-2008, after the WW2006-2007 crop, a satisfactory
410 match between measured and simulated accumulated N losses to the drainage could exclusively be explained from the reduced denitrification loss (Fig. 11). As mentioned above, soil N concentration in soil water sampled with suction cups was used for validation purposes. The soil water N concentration had similar behaviour before and after the calibration, except the dynamics were better matched after calibration (Fig. 12). During the WW2003-2004 crop drainage period, the calibrated model was able to depict the $25\,\mathrm{mg\,N\,L^{-1}}$ measured peak as well as the fluctuations from 2002 to 2004. However, both models underestimated
415 the N concentration substantially in the period after WW followed by FB 2007-2008. Again, these differences could not be explained by an overestimated high N uptake (cf. Fig. 10). Although the drainage input of N massively increased due to the change in denitrification, the simulated N concentration only improved nRMSE[%] 5%-point for the whole period, which is equal to $1\,\mathrm{mg\,N\,L^{-1}}$. Visual and mathematical inspection of the N concentration show, of course, a decent improvement on the soil N dynamics, but with this pronounced change in denitrification, the expected rise could be expected to be higher, if the
420 more available N was not transported further down to the lower soil matrix (Fig. 1a) as DM1 and DM2 macropores start either from the surface or from the bottom of the plow layer (A horizon). However, both are conceptually described to transport water and nutrients to the drainage system, and water build up is not allowed in the model. Besides, three other MM type macropores are present in this conceptual system with the possibility to transport water and solute: from surface to the bottom of the plow pan (MM1), from the surface to below the drain level at 150 cm depth (MM2) and from the bottom of the plow layer to below
425 the drain level at 150 cm depth (MM3).

[Figure 12 is about here]

The latter two have the capability to transport N from the surface/plow layer below the drain level, bypassing the entire B horizon. This limits the transport through the mentioned horizon by matrix flow. The conceptual description of deep macropores

points out another possible rapid transport route for N from the plow layer towards the groundwater. By comparing the mea-

430 sured suction cups samples with the simulated concentrations at 2 m depth, a remarkable 30 %-point decrease can be observed

in the nRMSE[%] and 0.3 nMAE performance measure (Fig. 13). Rosenbom et al. (2009) concluded that deep fractures might

result in deep leaching of agrochemicals and nutrient. However, these flow phenomena were outside the scope of the present

study.

[Figure 13 is about here]

435 **4  Conclusions**

This study aimed to evaluate, by using one-dimensional physically based root zone model DAISY (Hansen, 2002), the effect

of preferential transport and denitrification on leaching of nitrate to drainage during a 10-years period, as measured for an

agricultural clay till field included in the Danish Pesticide Leaching Assessment Programme (PLAP; Lindhardt et al. (2001);

web address: http://pesticidvarsling.dk). The results reveal a dominant effect on the leaching of nitrate through this clay till

440 field. A large amount of N (48% to 80% of the total N-loss to drainage) was preferentially transported via macropores to

drainage, regardless of the application method and concurrent occurrence of precipitation. The current standard denitrification

water reduction factor, fs, needed modification with a reduction of approximately 50% in the denitrification of the field from a

seasonal average of $75 \, \mathrm{kg\, N\, ha^{-1}}$ to $35 \, \mathrm{kg\, N\, ha^{-1}}$. The crop model provided acceptable results, and further studies are needed

to improve the simulation of N uptake in crops. Overall, this study delineates the importance of accounting for preferential

445 transport and coherent denitrification in the assessment of the leaching risk of nitrate to the aquatic environment.

*Author contributions.*  David Nagy(DN) carried out the development of the conceptualisation and methodology under the co-supervision of

Annette E. Rosenbom(AER) and Bo Vangsø Iversen(BVI) and main supervision of Finn Plauborg(FP). DN developed the model calibration

code, performed the simulations and prepared the manuscript with contributions from all co-authors. AER provided the PLAP experiment

data of Silstrup, whereas FP provided the corresponding climate data. AER and FP are responsible for the data curation of the experiment.

450 *Acknowledgements.*  The research was funded by Aarhus University. Aarhus University, Department of Agroecology and Geological Survey

of Denmark and Greenland, Department of Geochemistry provided all data from the Pesticide Leaching Assessment Programme (PLAP).

The data can be requested from Annette E. Rosenbom. email: aer@geus.dk

# References

Allen, R. G., Pereira, L. S., Raes, D., and Smith, M.: Crop evapotranspiration-guidelines for computing crop water requirements-fao irrigation
455     and drainage paper 56, FAO, Rome, 300, D05 109, 1998.

Ardia D., Mullen K.M., P. B. U. J.: 'Deoptim': An r package for global optimization by differential evolution., http://www.jstatsoft.org/v40/
i06/, 2016.

Bergstrom, L.: Leaching of dichlorprop and nitrate in structured soil, Environ Pollut, 87, 189–95, https://doi.org/10.1016/0269-
7491(94)p2606-a, https://www.ncbi.nlm.nih.gov/pubmed/15091593, 1995.

460 Blann, K. L., Anderson, J. L., Sands, G. R., and Vondracek, B.: Effects of agricultural drainage on aquatic ecosystems: A review, Criti-
cal Reviews in Environmental Science and Technology, 39, 909–1001, https://doi.org/10.1080/10643380801977966, <GotoISI>://WOS:
000272596000001, 2009.

Brady, N., Weil, R., Brady, N., and Weil, R.: Soil colloids: Seat of soil chemical and physical acidity, 2008.

Campolongo, F., Cariboni, J., and Saltelli, A.: An effective screening design for sensitivity analysis of large models, Environmental Modelling
465     & Software, 22, 1509–1518, https://doi.org/10.1016/j.envsoft.2006.10.004, <GotoISI>://WOS:000247403800013, 2007.

Cheng, J. H., Zhang, H. J., Zhang, Y. Y., Chen, Y. Z., and Wang, B. Y.: Characteristics of preferential flow paths and their impact on nitrate
nitrogen transport on agricultural land, Polish Journal of Environmental Studies, 23, 1959–1964, <GotoISI>://WOS:000347510700008,
2014.

Ciric, C., Ciffroy, P., and Charles, S.: Use of sensitivity analysis to identify influential and non-influential parameters within an
470     aquatic ecosystem model, Ecological Modelling, 246, 119–130, https://doi.org/10.1016/j.ecolmodel.2012.06.024, <GotoISI>://WOS:
000310255100013, 2012.

Criss, R. E. and Winston, W. E.: Do nash values have value? Discussion and alternate proposals, Hydrological Processes, 22, 2723–2725,
https://doi.org/10.1002/hyp.7072, <GotoISI>://WOS:000257954400029, 2008.

EEC: Council directive 91/676/eec of 12 december 1991 concerning the protection of waters against pollution caused by nitrates from
475     agricultural sources oj l 375, 1991.

Ernstsen, V., Olsen, P., and Rosenbom, A. E.: Long-term monitoring of nitrate transport to drainage from three agricultural clayey
till fields, Hydrology and Earth System Sciences, 19, 3475–3488, https://doi.org/10.5194/hess-19-3475-2015, <GotoISI>://WOS:
000360653600010, 2015.

Grundmann, G. L. and Rolston, D. E.: A water function approximation to degree of anaerobiosis associated with denitrification, Soil Science,
480     144, 437–441, https://doi.org/10.1097/00010694-198712000-00008, <GotoISI>://WOS:A1987L671100008, 1987.

Gupta, H. V., Kling, H., Yilmaz, K. K., and Martinez, G. F.: Decomposition of the mean squared error and nse performance criteria:
Implications for improving hydrological modelling, Journal of Hydrology, 377, 80–91, https://doi.org/10.1016/j.jhydrol.2009.08.003,
<GotoISI>://WOS:000271125800009, 2009.

Hansen, S.: Daisy, a flexible soil-plant-atmosphere system model, Report. Dept. Agric, 2002.

485 Hansen, S., Jensen, H., Nielsen, N., and Swenden, H.: Daisy: A soil plant system model. Danish simulation model for transformation and
transport of energy and matter in the soil plant atmosphere system, The National Agency for Environmental Protection, p. 369, 1990.

Hansen, S., Abrahamsen, P., and Petersen, C.: Daisy 2d simulation of silstrup and estrup, Report, University of Copenhagen, 2010a.

Hansen, S., Petersen, C., Abrahamsen, P., Nielsen, M., and Mollerup, M.: Daisy 2d simulation of rørrendegård, Technical report, University
of Copenhagen, 2010b.

490    Hansen, S., Abrahamsen, P., Petersen, C. T., and Styczen, M.: Daisy: Model use, calibration, and validation, Transactions of the Asabe, 55, 1315–1333, <GotoISI>://WOS:000309089900017, 2012a.

Hansen, S., Petersen, C., Mollerup, M., Abrahamsen, P., Gjettermann, B., Nielsen, M., Styczen, M., Poulsen, R., Lørup, J., Yamagata, K., and Butts, M.: Flerdimensional modellering af vandstrømning og stoftransport i de øverste 1-2m af jorden i systemer med markdræn, Report, University of Copenhagen & DHI, 2012b.

495    Hansson, B. G. and Hokfelt, B.: Long term treatment of moderate hypertension with penbutolol (hoe 893d). I. Effects on blood pressure, pulse rate, catecholamines in blood and urine, plasma renin activity and urinary aldosterone under basal conditions and following exercise, Eur J Clin Pharmacol, 9, 9–19, https://doi.org/10.1007/bf00613424, https://www.ncbi.nlm.nih.gov/pubmed/9298, 1975.

Heinen, M.: Simplified denitrification models: Overview and properties, Geoderma, 133, 444–463, https://doi.org/10.1016/j.geoderma.2005.06.010, <GotoISI>://WOS:000238981300024, 2006.

500    Hofstra, N. and Bouwman, A. F.: Denitrification in agricultural soils: Summarizing published data and estimating global annual rates, Nutrient Cycling in Agroecosystems, 72, 267–278, https://doi.org/10.1007/s10705-005-3109-y, <GotoISI>://WOS:000233044000006, 2005.

Hooghoudt, S. B.: Algemene beschouwing van het probleem van de detailontwatering en de infiltratie door middel van parallel loopende drains, greppels, slooten en kanalen, 1940.

Jabloun, M.: Cereal crop productivity and nitrogen cycling under climate change : Phd dissertation, Aarhus University, Department of
505    Agroecology, Foulum, https://www.statsbiblioteket.dk/au/#/search?query=recordID%3A%22sb_6242296%22, 2015.

Jabloun, M., Li, X., Olesen, J. E., Schelde, K., and Tao, F.: Rdaisy: A comprehensive modelling framework for automated calibration, sensitivity and uncertainty analysis of the daisy model, Modelling Climate Change Impacts on Crop Production for Food Security, 2014.

Jain, A. K. and Dubes, R. C.: Algorithms for clustering data, vol. 6, Prentice hall Englewood Cliffs, 1988.

Jarvis, S. C., Stockdale, E. A., Shepherd, M. A., and Powlson, D. S.: Nitrogen mineralization in temperate agricultural soils: Processes and
510    measurement, in: Advances in agronomy volume 57, edited by Sparks, D. L., vol. 57 of *Advances in agronomy*, pp. 187–235, Academic Press, https://doi.org/10.1016/s0065-2113(08)60925-6, http://www.sciencedirect.com/science/article/pii/S0065211308609256, 1996.

Klint, K. E. S. and Gravesen, P.: Fractures and biopores in weichselian clayey till aquitards at flakkebjerg, denmark, Hydrology Research, 30, 267–284, https://doi.org/10.2166/nh.1999.0015, http://dx.doi.org/10.2166/nh.1999.0015, 1999.

Knudsen, L., Østergaard, H., and E., S.: Kvælstof - et næringsstof og et miljøproblem, Report, Landskontoret for Planteavl, 2000.

515    Larsson, M. H. and Jarvis, N. J.: A dual-porosity model to quantify macropore flow effects on nitrate leaching, Journal of Environmental Quality, 28, 1298–1307, https://doi.org/10.2134/jeq1999.00472425002800040034x, <GotoISI>://WOS:000081345400032, 1999.

Lind, A. M.: Denitrification in the root zone, Tidsskrift for Planteavl, 84, 101–110, https://www.cabdirect.org/cabdirect/abstract/19801957950, 1980.

Lindhardt, B., Abildtrup, C., Vosgerau, H., Olsen, P., Torp, S., Iversen, B. V., Jørgensen, J. O., Plauborg, F., Rasmussen, P., and Gravesen, P.:
520    The danish pesticide leaching assessment programme: Site characterization and monitoring design, Report, Geological Survey of Denmark and Greenland, 2001.

Manevski, K., Borgesen, C. D., Li, X., Andersen, M. N., Abrahamsen, P., Hu, C., and Hansen, S.: Integrated modelling of crop production and nitrate leaching with the daisy model, MethodsX, 3, 350–63, https://doi.org/10.1016/j.mex.2016.04.008, https://www.ncbi.nlm.nih.gov/pubmed/27222825, 2016.

525    Manzoni, S. and Porporato, A.: Soil carbon and nitrogen mineralization: Theory and models across scales, Soil Biology and Biochemistry, 41, 1355–1379, https://doi.org/10.1016/j.soilbio.2009.02.031, <GotoISI>://WOS:000267775300001, 2009.

Mohanty, B. P., Bowman, R. S., Hendrickx, J. M. H., Simunek, J., and van Genuchten, M. T.: Preferential transport of nitrate to a tile drain in an intermittent-flood-irrigated field: Model development and experimental evaluation, Water Resources Research, 34, 1061–1076, https://doi.org/10.1029/98wr00294, <GotoISI>://WOS:000073407600011, 1998.

530  Mollerup, M.: Daisy 2d numerics, http://daisy.ku.dk/publications/Num2D-v2.pdf, 2010.

Morris, M. D.: Factorial sampling plans for preliminary computational experiments, Technometrics, 33, 161–174, https://doi.org/10.1080/00401706.1991.10484804, <GotoISI>://WOS:A1991FJ19800006, 1991.

Mualem, Y.: A new model for predicting the hydraulic conductivity of unsaturated porous media, Water resources research, 12, 513–522, 1976.

535  Muleta, M. K.: Model performance sensitivity to objective function during automated calibrations, Journal of hydrologic engineering, 17, 756–767, 2011.

Nagy, D., Rosenbom, A. E., Iversen, B. V., Jabloun, M., and Plauborg, F.: Estimating the degree of macropore flow to drainage at an agricultural clay till field for a 10-years period, Hydrology and Earth System Sciences, https://doi.org/10.5194/hess-2019-665, discussion paper, 2019.

540  Reddy, K. R. and Ronald, D. D.: Biogeochemistry of wetlands: Science and applications, vol. I, book section 8, CRC Press, 2008.

Richards, L. A.: Capillary conduction of liquids through porous mediums, Physics, 1, 318–333, https://doi.org/10.1063/1.1745010, <GotoISI>://WOS:000202861500042, 1931.

Rodrigo, A., Recous, S., Neel, C., and Mary, B.: Modelling temperature and moisture effects on c–n transformations in soils: Comparison of nine models, Ecological Modelling, 102, 325–339, https://doi.org/10.1016/s0304-3800(97)00067-7, http://www.sciencedirect.com/science/article/pii/S0304380097000677, 1997.

Rosenbom, A. E., Therrien, R., Refsgaard, J. C., Jensen, K. H., Ernstsen, V., and Klint, K. E.: Numerical analysis of water and solute transport in variably-saturated fractured clayey till, J Contam Hydrol, 104, 137–52, https://doi.org/10.1016/j.jconhyd.2008.09.001, https://www.ncbi.nlm.nih.gov/pubmed/18926594, 2009.

Simunek, J., Jarvis, N. J., van Genuchten, M. T., and Gardenas, A.: Review and comparison of models for describing non-equilibrium and preferential flow and transport in the vadose zone, Journal of Hydrology, 272, 14–35, <GotoISI>://WOS:000181147900003, 2003.

Singh, J., Knapp, H. V., Arnold, J. G., and Demissie, M.: Hydrological modeling of the iroquois river watershed using hspf and swat, Journal of the American Water Resources Association, 41, 343–360, https://doi.org/10.1111/j.1752-1688.2005.tb03740.x, https://onlinelibrary.wiley.com/doi/abs/10.1111/j.1752-1688.2005.tb03740.x, 2005.

Van Genuchten, M. T.: A closed-form equation for predicting the hydraulic conductivity of unsaturated soils, Soil science society of America journal, 44, 892–898, 1980.

Vries, F. P. d.: Simulation of ecophysiological processes of growth in several annual crops, vol. 29, Int. Rice Res. Inst., 1989.

**List of Figures**

**Figure 1.** Topography and field instrumentation of the Silstrup field.

**Figure 2.** Crop rotations, **a)** Precipitation and cumulative drainage per season, **b)** Nitrate-N concentration in water abstracted from suction cups at 1 m depth and applications of mineral N fertilizer and injection of slurry (organic) **c)** Nitrate-N concentration in drainage water and cumulative flux of nitrate-N in drainage per season.
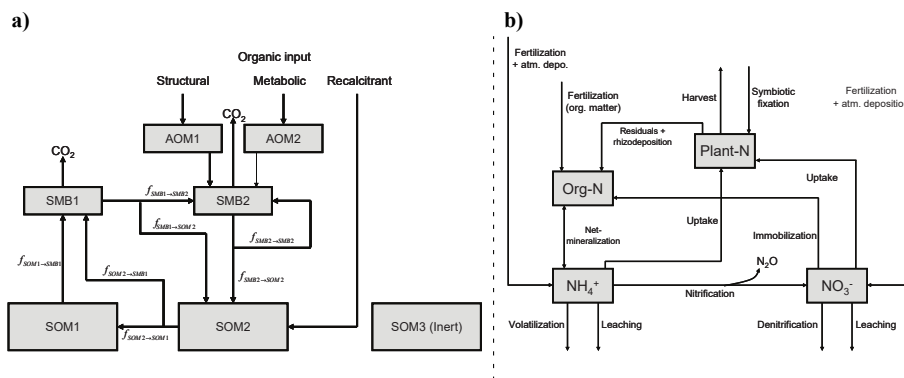
**Figure 3. a)** Schematic overview of the soil organic matter model included in the Daisy model. AOM = added organic matter, SMB = soil microbial biomass, and SOM = native soil organic matter; fx = partitioning coefficient. The inert SOM3 pool does not interact with the rest of the system. **b)** Schematic overview of the nitrogen model in Daisy (Hansen et al., 2012a).
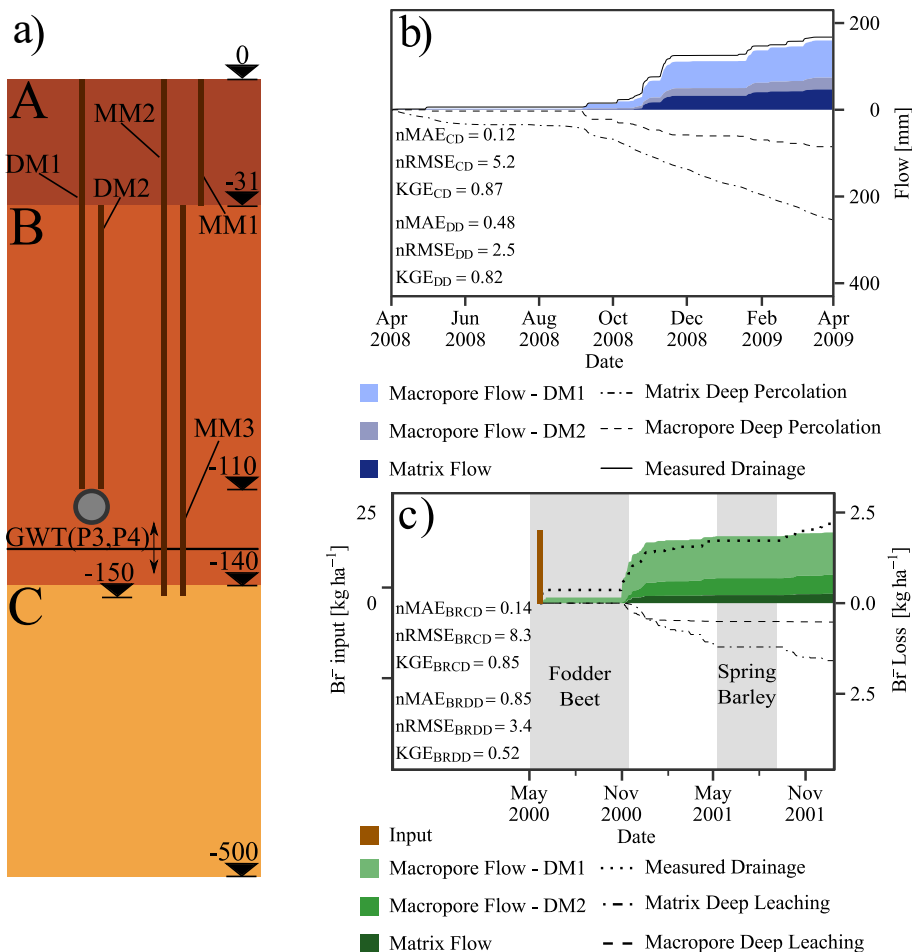
**Figure 4. a)** Hydrological concept: DM – Drainage ended macropore, MM – Matrix ended macropore; **b)** Simulated accumulated drainage flow originating from the matrix and macropore domain with the corresponding nMAE, nRMSE[%] and KGE for 2008-2009; **c)** Simulated accumulated Br⁻ transport to drainage from matrix and macropore domain and measured Br⁻ transport in the drain flow with the corresponding nMAE, nRMSE[%] and KGE for 2000-2001. Subscripts: *DC* – Cumulative Drainage [mm], *DD* – Drainage Dynamics [mm h$^{-1}$], BRDD – Br Drainage transport dynamics [kg Br$^-$ ha$^{-1}$ h$^{-1}$], BRDC – Cumulative Br⁻ transport [kg Br$^-$ ha$^{-1}$] (Nagy et al., 2019).
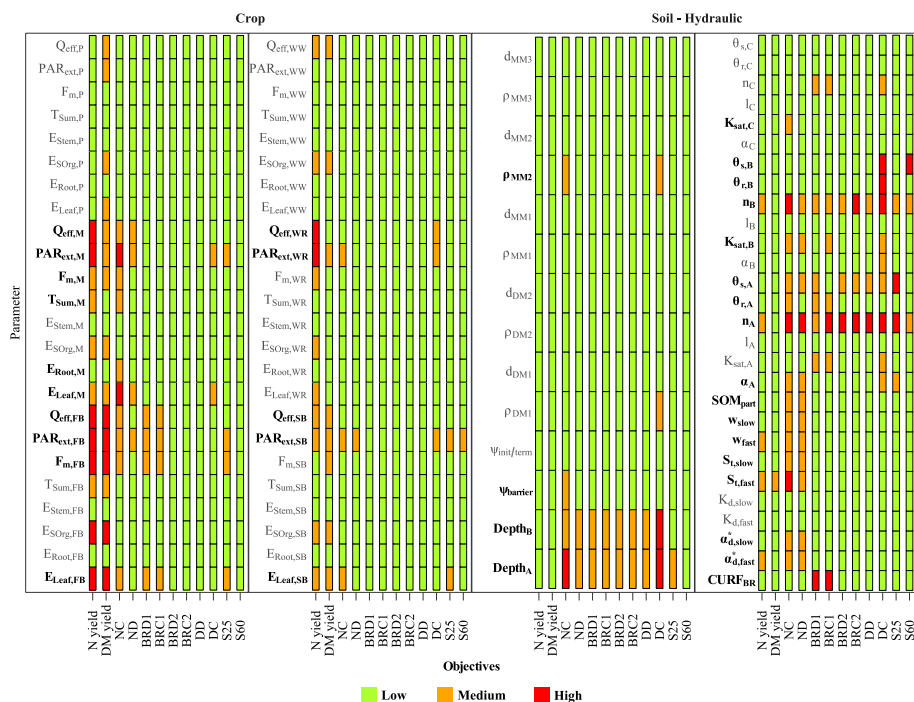
**Figure 5.** Sensitivity groups of selected CP and SH input parameters in regards to the 12 objective functions (Black – Sensitive parameters, Gray – non-sensitive parameters).
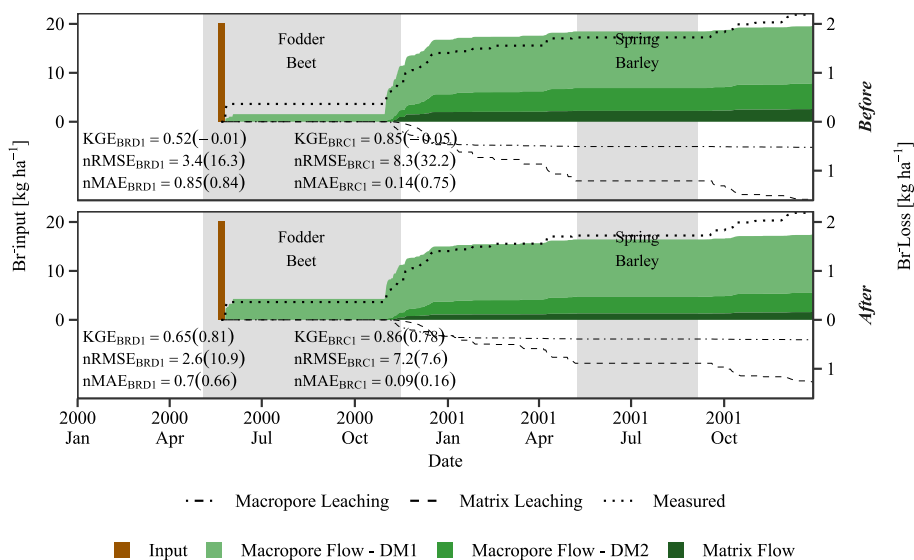
**Figure 6.** Simulated accumulated Br⁻ transport to drainage from matrix and macropore domain and measured Br⁻ transport in the drain flow. Objectives *BRD1* and *BRC1* with the corresponding nMAE, nRMSE[%], and KGE for 2000-2001 before and after the calibration. In parenthesis, the performance for the objectives *BRD2* and *BRC2*.
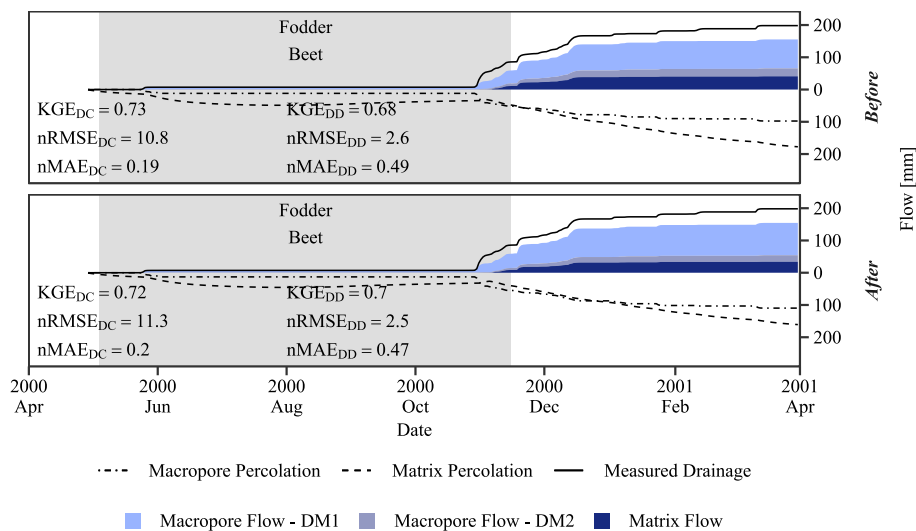
**Figure 7.** Simulated accumulated water transport from the matrix and macropore domain and measured drain flow. Objective *DD* and *DC* with the corresponding nMAE, nRMSE[%] and KGE for 2000-2001, before and after the calibration.
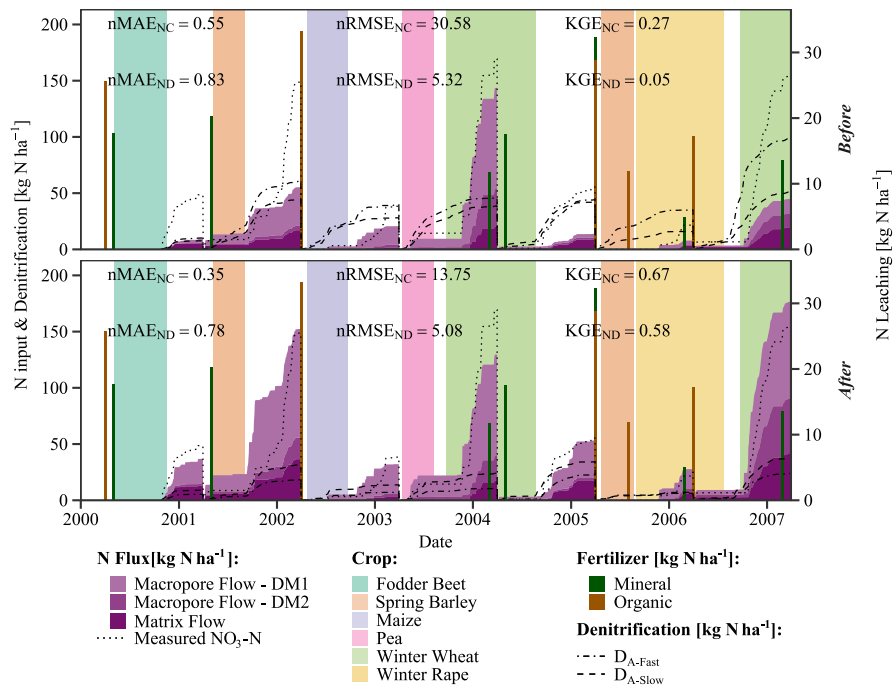
**Figure 8.** Simulated seasonally accumulated NO₃-N transport from matrix and macropore domain and accumulated measured NO₃-N in the drainage. Included in the objectives *ND*, NC with the corresponding nMAE, nRMSE[%] and KGE for calibration period of 2000-2007, before and after the calibration and additionally shown the seasonally accumulated denitrification from fast and slow pools.
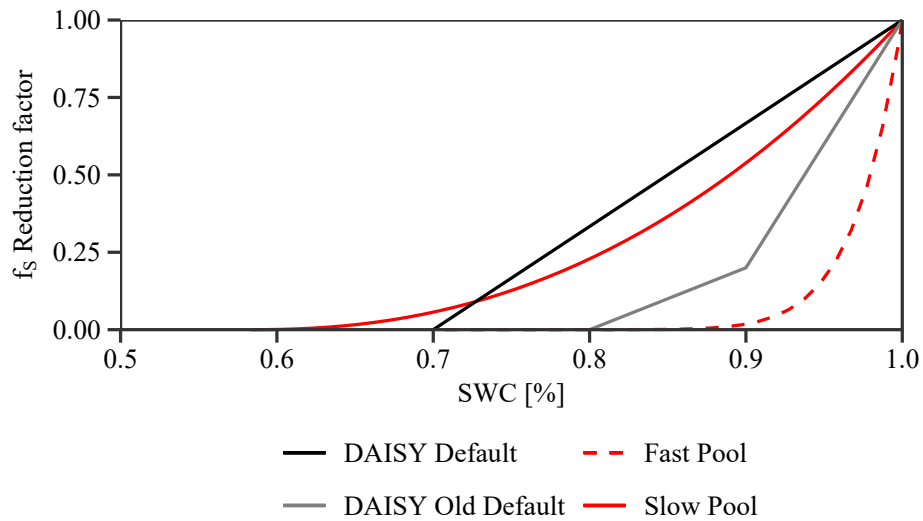
**Figure 9.** Default (Hansen, 2002) and old default (Hansen et al., 1990) water reduction factor of denitrification of DAISY and the calibrated water reduction factor of denitrification for the slow and fast pools.
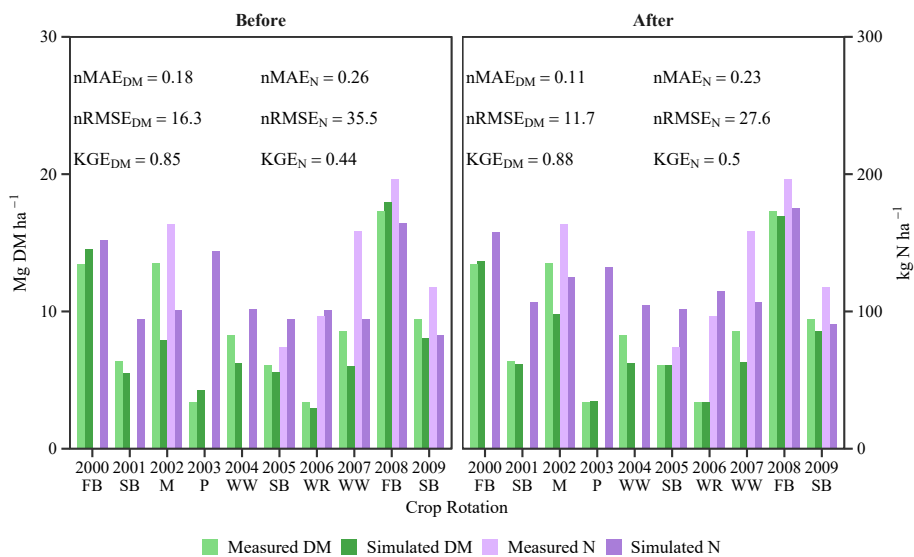
**Figure 10.** Harvested DM and N of the storage organ before and after the calibration. For the objectives *DM yield* and *N yield*, the performance measures nMAE, nRMSE[%] and KGE.
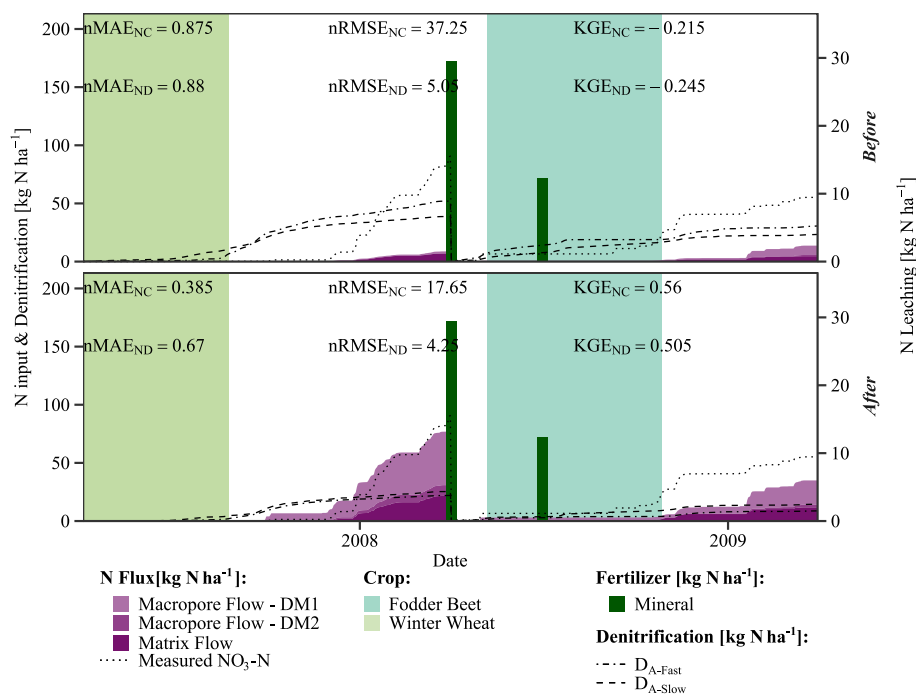
**Figure 11.** Simulated seasonally accumulated NO$_3$-N transport from matrix and macropore domain and measured NO$_3$-N in the drainage with the corresponding nMAE, nRMSE[%], and KGE for the objectives *ND* and *NC* for the period of 2008-2009 before and after the calibration. Additionally, the seasonally accumulated denitrification from fast and slow pools is plotted.
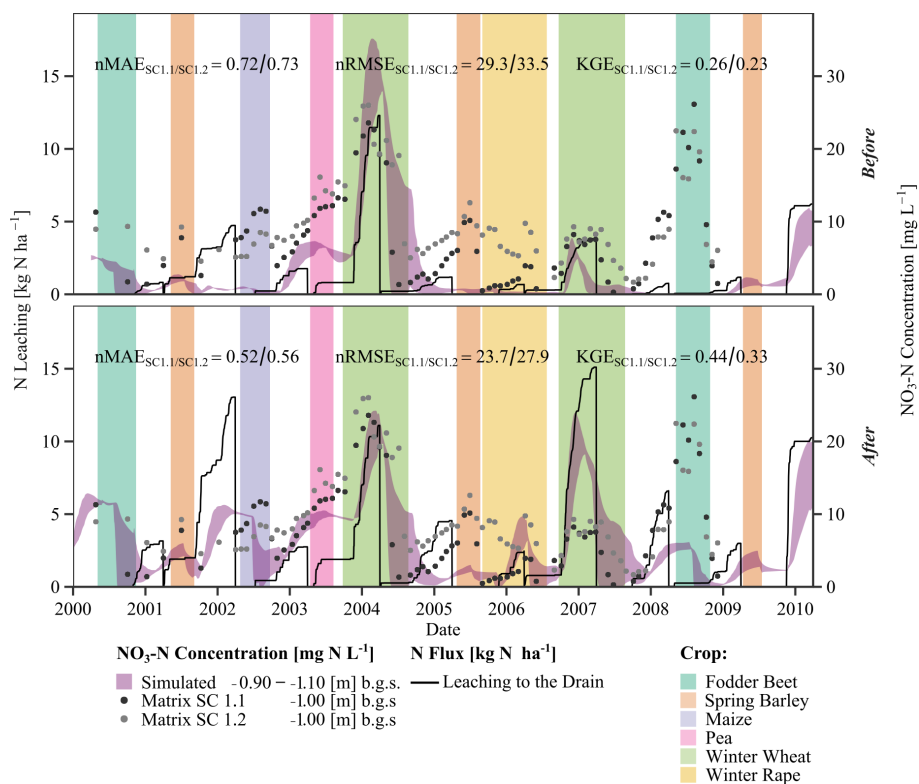
**Figure 12.** Simulated and measured soil $NO_3$-N concentration 1 m depth from 2000 to 2010 **a)** before and **b)** after the calibration. Performance measures calculated for the entire period for the simulated and measured N concentrations at the two replicate depths (SC1.1 and SC1.2).
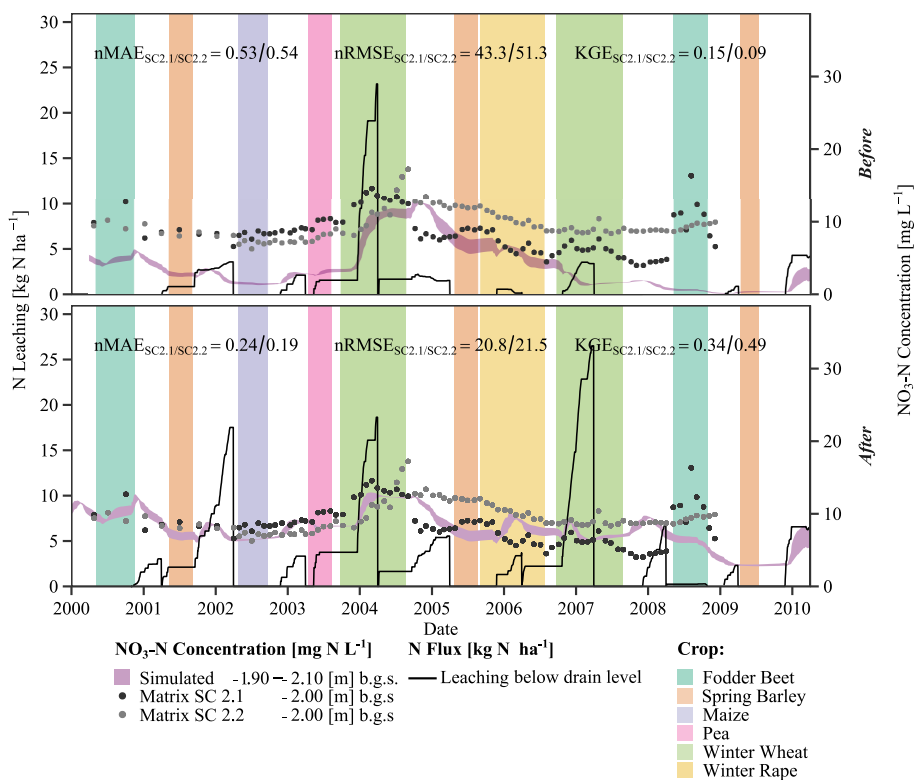
**Figure 13.** Simulated and measured soil $NO_3$-N concentration at 2 m depth from 2000 to 2010 before and after the calibration. Performance measures calculated for the entire period for the simulated and measured N concentrations at the two replicate depths (SC2.1 and SC2.2).

**List of Tables**

**Table 1.** Initial van Genuchten - Mualem parameters for the matrix domain of A, B, and C (from Nagy et al. (2019)). $\theta_r$ is the residual water content, $\theta_s$ is the saturated water content, $\alpha$ and $n$ are the retention curve shape parameter, $K_{sat}$ saturated hydraulic conductivity, $l$ is the pore connectivity parameter in the Mualem equation.

| $\theta_{r,A}$ cm$^3$ cm$^{-3}$ | $\theta_{r,B}$ cm$^3$ cm$^{-3}$ | $\theta_{r,C}$ cm$^3$ cm$^{-3}$ | $\theta_{s,A}$ cm$^3$ cm$^{-3}$ | $\theta_{s,B}$ cm$^3$ cm$^{-3}$ | $\theta_{s,C}$ cm$^3$ cm$^{-3}$ | $l_A$ - | $l_B$ - | $l_C$ - |
|---|---|---|---|---|---|---|---|---|
| 0.01 | 0.013 | 0.01 | 0.4063 | 0.3783 | 0.2938 | 0.5 | 0.5 | 0.5 |
| $K_{sat,A}$ cm h$^{-1}$ | $K_{sat,B}$ cm h$^{-1}$ | $K_{sat,C}$ cm h$^{-1}$ | $\alpha_A$ - | $\alpha_B$ - | $\alpha_C$ - | $n_A$ - | $n_B$ - | $n_C$ - |
| 10.71 | 0.03 | 0.28 | 0.051 | 0.0045 | 0.001 | 1.186 | 1.2005 | 1.2154 |

**Table 2.** Initial parameters for the macropore domain of DM1, DM2 and MM1, MM2, MM3 (from (Nagy et al., 2019). $Depth$ is the depth of the denoted horizon, $\psi_{init/term}$ is the initiating – terminating pressure of the macropore flow, $\psi_{barrier}$ is the required pressure difference between the macropore and matrix, $\rho$ is the density of the denoted macropore type, and $d$ is the diameter of the denoted macropore type.

| $Depth_A$ | $Depth_B$ | $\psi_{init/term}$ | $\psi_{barrier}$ | $\rho_{DM1}$ | $\rho_{DM2}$ | $d_{DM1}$ | $d_{DM2}$ |
|---|---|---|---|---|---|---|---|
| cm | cm | cm | cm | m$^{-2}$ | m$^{-2}$ | mm | mm |
| -39.29 | -140 | -2.93 | -5 | 5.489 | 12.643 | 3 | 3 |
| | $\rho_{mm1}$ | $\rho_{mm2}$ | $\rho_{mm3}$ | $d_{mm1}$ | $d_{mm2}$ | $d_{mm3}$ | |
| | m$^{-2}$ | m$^{-2}$ | m$^{-2}$ | mm | mm | mm | |
| | 100 | 11.5 | 11.5 | 2 | 3 | 3 | |

**Table 3.** Initial parameters, taken from DAISY library (Hansen et al., 2012a) for crop models for the different crops in rotation (FB – Fodder Beet, M – Maize, P – Pea, SB – Spring Barley, WR – Winter Rape, WW – Winter Wheat). E parameters are conversion efficiency (growth respiration). $F_m$ is the maximum assimilation rate. $PAR_{ext}$ is Photosynthetic Active Radiation extinction coefficient. $Q_{eff}$ quantum efficiency at low light. $T_{sum}$ is the temperature sum at emergence of the crop.

| Parameter | FB | M | P | SB | WR | WW |
|-----------|------|------|------|------|------|------|
| $E_{Root}$ | 0.69 | 0.78 | 0.69 | 0.69 | 0.69 | 0.69 |
| $E_{Stem}$ | 0.66 | 0.69 | 0.66 | 0.66 | 0.66 | 0.66 |
| $E_{Leaf}$ | 0.66 | 0.75 | 0.7 | 0.68 | 0.68 | 0.68 |
| $E_{SOrg}$ | 0.7 | 0.8 | 0.55 | 0.7 | 0.5 | 0.7 |
| $T_{sum}$ | 250 | 180 | 100 | 100 | 180 | 100 |
| $F_m$ | 4 | 6.5 | 4 | 5 | 5.25 | 5.59 |
| $PAR_{ext}$ | 0.67 | 0.8 | 0.3 | 0.6 | 0.7 | 0.6 |
| $Q_{eff}$ | 0.06 | 0.04 | 0.04 | 0.04 | 0.05 | 0.05 |

**Table 4.** Initial parameters for denitrification, Br⁻ uptake, and SOM.

| $CURF_{BR}$ | $\alpha_d^*$ | $K_d$ | $SOM_{ratio}$ | $S_t$ | $w$ |
|---|---|---|---|---|---|
| - | $(\mathrm{g\,NO_3-N\,h^{-1}})(\mathrm{g\,CO_2-C\,h^{-1}})^{-1}$ | - | - | - | - |
| 0.2 | 0.1 | 0.020833 | 1 | 0.7 | 1 |

**Table 5.** Calibrated objectives and the normalized standard deviation of the measurements for the calibration period of 2000-2007. Initial objective values shown in brackets. nMAE – normalized mean absolute error, $nSD_{mean}$ – SD normalized by mean observation, nRMSE[%] – normalized root mean squared error, nSD[%] – SD normalized by the maximum deviation of the observation, KGE – Kling-Gupta Efficiency.

| Objectives | nMAE | | $nSD_{mean}$ | nRMSE[%] | | nSD[%] | KGE | |
|---|---|---|---|---|---|---|---|---|
| N yield | 0.23 | (0.26) | 0.37 | 27.6 | (35.5) | 41.4 | 0.5 | (0.44) |
| DM yield | 0.11 | (0.18) | 0.54 | 11.7 | (16.3) | 34.9 | 0.88 | (0.85) |
| ND | 0.7 | (0.81) | 3.49 | 4.3 | (4.66) | 5.22 | 0.56 | (-0.03) |
| NC | 0.31 | (0.67) | 1.18 | 13.96 | (31.64) | 34.5 | 0.68 | (0.08) |
| BRD1 | 0.7 | (0.87) | 4.28 | 2.6 | (3.3) | 3.8 | 0.65 | (0.61) |
| BRC1 | 0.09 | (0.2) | 0.55 | 7.2 | (12.4) | 30.6 | 0.86 | (0.73) |
| BRD2 | 0.66 | (0.74) | 2.5 | 10.9 | (13.9) | 19.5 | 0.81 | (0.16) |
| BRC2 | 0.16 | (0.65) | 1.97 | 7.6 | (27.9) | 38.5 | 0.78 | (0.09) |
| DD | 0.53 | (0.52) | 3.5 | 2.6 | (2.66) | 4.44 | 0.74 | (0.72) |
| DC | 0.13 | (0.12) | 1.17 | 5.4 | (5.22) | 34.82 | 0.89 | (0.89) |
| S25 | 0.12 | (0.1) | 0.18 | 19.36 | (17.04) | 25.24 | 0.64 | (0.71) |
| S60 | 0.04 | (0.05) | 0.04 | 29.4 | (35.26) | 20.78 | 0.09 | (0.03) |
| MEAN | 0.315 | (0.43) | 1.65 | 11.89 | (17.15) | 24.48 | 0.67 | (0.44) |

**Table 6.** Calibrated SH/CP parameters. Initial parameter values shown in brackets.

| $\theta_{r,A}$ | $\theta_{r,B}$ | $\theta_{s,A}$ | $\theta_{s,B}$ | $\alpha_A$ | $n_A$ | $n_B$ |
|---|---|---|---|---|---|---|
| 0.01 | 0.013 | 0.39 | 0.39 | 0.053 | 1.231 | 1.176 |
| (0.01) | (0.013) | (0.41) | (0.38) | (0.051) | (1.186) | (1.201) |
| $K_{sat,B}$ | $K_{sat,C}$ | $\psi_{barrier}$ | $\rho_{MM3}$ | $SOM_{ratio}$ | $Depth_A$ | $Depth_B$ |
| 0.029 | 0.285 | -5.15 | 11.72 | 1.67 | -35.4 | -141.4 |
| (0.03) | (0.28) | (-5) | (11.5) | (1) | (-39.3) | (-140) |
| $\alpha^*_{d,fast}$ | $\alpha^*_{d,slow}$ | $S_{t,fast}$ | $w_{fast}$ | $S_{t,slow}$ | $w_{slow}$ | |
| 0.071 | 0.154 | 0.71 | 9.6 | 0.58 | 2.3 | |
| (0.1) | (0.1) | (0.7) | (1) | (0.7) | (1) | |
| $E_{Leaf,FB}$ | $E_{SOrg,FB}$ | $F_{m,FB}$ | $PAR_{ext,FB}$ | $Q_{eff,FB}$ | $E_{Leaf,SB}$ | $PAR_{ext,SB}$ |
| 0.76 | 0.62 | 4.61 | 0.58 | 0.07 | 0.79 | 0.52 |
| (0.66) | (0.7) | (4.00) | (0.67) | (0.06) | (0.68) | (0.60) |
| $Q_{eff,SB}$ | $E_{Leaf,M}$ | $E_{Root,M}$ | $T_{sum,M}$ | $F_{m,M}$ | $PAR_{ext,M}$ | $Q_{eff,M}$ |
| 0.05 | 0.86 | 0.69 | 156.75 | 7.57 | 0.76 | 0.05 |
| (0.04) | (0.75) | (0.78) | (180) | (6.50) | (0.80) | (0.04) |
| $PAR_{ext,WR}$ | $Q_{eff,WR}$ | $CURF_{BR}$ | | | | |
| 0.57 | 0.06 | 0.0034 | | | | |
| (0.70) | (0.05) | (0.0) | | | | |